

See discussions, stats, and author profiles for this publication at: <https://www.researchgate.net/publication/237146468>

Efficiency of Noncoherent Photon Upconversion by Triplet–Triplet Annihilation: The C60 Plus Anthanthrene System and the Importance of Tuning the Triplet Energies

ARTICLE *in* THE JOURNAL OF PHYSICAL CHEMISTRY A · JUNE 2013

Impact Factor: 2.69 · DOI: 10.1021/jp404587u · Source: PubMed

CITATIONS

9

READS

135

4 AUTHORS, INCLUDING:



Sunish K Sugunan

Mahatma Gandhi University

5 PUBLICATIONS 63 CITATIONS

SEE PROFILE

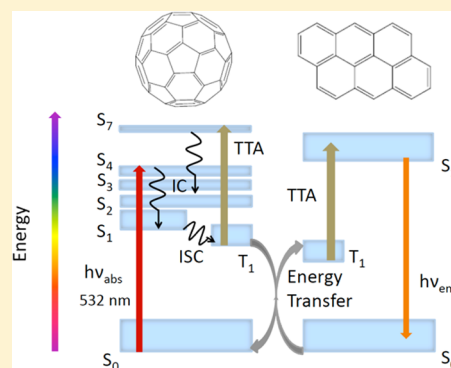
Efficiency of Noncoherent Photon Upconversion by Triplet–Triplet Annihilation: The C₆₀ Plus Anthanthrene System and the Importance of Tuning the Triplet Energies

Sunish K. Sugunan,^{*,§} Chelsea Greenwald, Matthew F. Paige,^{*} and Ronald P. Steer^{*}

Department of Chemistry, University of Saskatchewan, Saskatoon, SK Canada S7N 5C9

S Supporting Information

ABSTRACT: As part of a continuing effort to find noncoherent photon upconversion (NCPU) systems with improved energy conversion efficiencies, the photophysics of the blue emitter, anthanthrene (An), and the fullerene absorber–sensitizer, C₆₀, have been examined by both steady-state and pulsed laser techniques. An is a promising candidate for NCPU by homomolecular triplet–triplet annihilation (TTA) because its triplet state lies $\sim 800\text{ cm}^{-1}$ below the triplet energy of the C₆₀ donor (thereby improving efficiency by reducing back triplet energy transfer), and its fluorescent singlet state lies in near resonance with double its triplet energy (thus minimizing thermal energy losses in the annihilation process). In fluid solution, efficient triplet–triplet donor–acceptor energy transfer is observed, and rate constants for homomolecular TTA in the An acceptor are estimated to approach the diffusion limit. NCPU is also observed in An + C₆₀ in poly(methylmethacrylate) thin films.



INTRODUCTION

Noncoherent photon upconversion (NCPU) realized by triplet–triplet annihilation (TTA) has recently re-emerged as an active area of research owing to the potential for its use in a variety of practical photon-initiated processes and optoelectronic devices.^{1–10} In particular, both NCPU and singlet fission¹¹ show significant promise of providing a means to circumvent the fundamental Shockley–Queisser efficiency limitations¹² that apply to single-threshold photovoltaic devices.

The basis for NCPU in organic molecular systems was first established through the observation of delayed fluorescence (DF) arising from TTA in solution. Anti-Stokes-shifted DF (i.e., NCPU) can arise following either (i) photon absorption by and efficient intersystem crossing in an organic donor having a relatively small singlet–triplet splitting, followed by triplet energy transfer to and TTA in an acceptor having a large singlet–triplet splitting, or (ii) photon absorption and subsequent homomolecular TTA in a single molecular system in which a more highly excited fluorescent electronic state is the product state of the annihilation. Both formulations have been explored, although reports for systems based on process (i) are much more numerous.¹³

We have recently demonstrated that upconverted emission from the S₂ states of d⁰ and d¹⁰ metalloporphyrins can result from type (ii) homomolecular TTA in both solution^{14,15} and polymer thin films.¹⁶ Although the higher-energy singlet electronic states populated by this process are short-lived, a substantial fraction of their pooled photon energy can nevertheless be captured via electron transfer or electronic energy transfer on a subpicosecond time scale. Both electron and energy transfer can occur from the S₂ states of

metalloporphyrins with the required ultrafast rates in suitable tethered dyads^{17,18} or in noncovalently bound donor–acceptor aggregates,^{15,19,20} thus offering the possibility of utilizing sub-band-gap solar photons in photovoltaics. In particular, we have demonstrated both ultrafast electron transfer in Soret-excited zinc porphyrins noncovalently bound to both fullerenes¹⁹ and selected aromatic polypyridines²⁰ and also ultrafast S₂–S₂ electronic energy transfer in tethered azulene–porphyrin dyads¹⁷ and in zinc porphyrin-free base porphyrin dendrimers.²¹

Our observation of subpicosecond electron transfer in a Soret-excited zinc tetraphenylporphyrin–C₆₀ 1:1 complex in solution has encouraged us to explore the NCPU possibilities offered by more robust molecules possessing higher-energy singlet states that can be accessed by homomolecular TTA. It is now well-established that photoexcitation of the simple fullerenes produce long-lived T₁ states with near-unit quantum efficiency.^{22–25} Homomolecular TTA occurs in these systems by what is now understood to be a standard mechanism that has been described in some detail. However, the identity of the initially excited singlet state resulting from TTA in these simple fullerene systems has not been established. Previous studies by Nickel²⁶ suggest that when several excited singlet electronic states are energetically accessible via the triplet–triplet interaction, the product state most likely to be populated and observed is the one nearest in resonance with the largest transition moment to the ground state.

Received: May 8, 2013

Revised: June 10, 2013

Published: June 11, 2013

The relevant photophysical properties of C_{60} are summarized in Table 1. The lowest triplet (T_1) energy of C_{60} is similar to the triplet energy of ZnTPP (1.5 eV) and has a lifetime on the order of 0.1 ms,^{24,25} making it a useful candidate for either homomolecular NCPU or heteromolecular triplet–triplet^{27–29} energy transfer. However, owing to the size and high symmetry of the C_{60} molecule, a large number of gerade singlet excited electronic states exist in the 1.5–3.0 eV region, all of which are parity-forbidden for one-photon transitions from the ground 1A_g state.²⁷ Consequently, C_{60} absorbs only very weakly throughout most of the visible region of the spectrum and fluoresces with a very small quantum yield. The lowest-energy electric-dipole-allowed transition to a singlet state has been revealed in the fluorescence excitation spectrum of C_{60} in a neon matrix at 4 K and lies between 400 and 410 nm. This $^1T_{1u} \rightarrow ^1A_g$ transition peaks at 407 nm (3.04 eV) for C_{60} in toluene.²⁷ The energy of this state is slightly lower than double the energy of the lowest triplet state of C_{60} , which satisfies the energy conservation requirements of TTA. Thus, in principle, following Nickel's analysis,²⁶ this $^1T_{1u}$ state may be the initial product excited state of homomolecular TTA in C_{60} . Homogeneous line-broadening measurements place the lifetime of this state in the region of a few hundred femtoseconds,³⁰ at the short-lifetime limit for interchromophoric electron- or energy-transfer processes to compete with internal conversion to lower singlet states. Nevertheless, the possibility of utilizing a large fraction of the energy of two C_{60} triplets is highly intriguing.

Here, we begin a series of reports of TTA in the fullerenes by describing the use of excited C_{60} as an energy donor in a type (i) NCPU system in which anthanthrene (An) is the triplet acceptor and upconverter. With this system, we show that even a poor visible photon absorber such as C_{60} can achieve reasonable upconversion yields in solution and solid films if the sensitizer and upconverter are carefully chosen to attenuate triplet back-energy transfer and optimize the singlet product yield via TTA.

■ EXPERIMENTAL SECTION

C_{60} (99.9% purity) and toluene (HPLC grade, $\geq 99.9\%$ purity) were purchased from Sigma-Aldrich and were used as received. An (high purity, verified by GC/MS) was purchased from Accustandard and was used as received. The steady-state absorption and fluorescence spectra of C_{60} and An in solution closely resemble the spectra reported previously^{23,27,31–33} and showed that the samples were free of measurable impurities in the spectral ranges of interest. Poly(methylmethacrylate) (PMMA) was purchased from Polysciences, showed no fluorescent impurities when excited in the visible region of the spectrum, and was used as received.

Toluene was chosen as the solvent because NCPU is favored in nonpolar solvents¹⁴ and because it does not form charge-transfer complexes with C_{60} .¹⁹ All solution samples for the NCPU experiments were first purged with ultra-high-purity nitrogen for at least 45 min and were subsequently transferred to the degassing reservoir of a custom-made high-vacuum cuvette in a dry nitrogen environment in a glovebox. Finally, samples were degassed by at least 10 freeze–pump–thaw cycles using a grease-free high-vacuum line. Solid-state samples were prepared by sequential spin-coating of 50 μ L aliquots of C_{60} , An, and 2.0% PMMA in toluene 40 times onto a precleaned glass slide and assuming that spin-casting of each aliquot makes a single incremental thin film for the sample. These sample

slides were mounted as the front window on a triangular brass cell, with the sample facing the inner, evacuable side of the cell when connected to a grease-free high-vacuum line. These thin film samples were degassed under vacuum for at least 1 h prior to measurement. The emission measurements were made in the front face geometry with the excitation beam intercepting the sample at $\sim 32^\circ$, less than the critical angle of incidence.

Absorption measurements were carried out using a Cary 6000i (Agilent) spectrophotometer operating in dual beam mode. Spectra were taken in 0.1 cm \times 1.0 cm, 1.0 cm \times 1.0, or 5.0 cm \times 1.0 cm quartz cuvettes depending on the absorbance, usually with a band-pass of 2.0 nm and a data acquisition step size of 1.0 nm. Titration measurements to find possible aggregation between C_{60} and An were done with a band-pass of 0.1 nm and a step size of 0.1 nm. Solution-state emission measurements were carried out using a PTI Quantamaster spectrofluorometer. Samples were excited through the long path, and the fluorescence emission was collected through the short path of a 2 \times 10 mm quartz cuvette to partially circumvent the effects of fluorescence reabsorption. Emission spectral artifacts induced by solvent Raman scattering and fluorescence reabsorption by both C_{60} and An were corrected using procedures reported previously.^{14,34,35} TTA emission measurements in polymer thin films were carried using a custom-modified Spex Fluorolog spectrophotometer and the evacuable, front-face-illuminated cell described above. For TTA emission measurements in both solution and the solid state, a low-power, frequency-doubled 532 nm cw Nd:YAG laser (WSTech, TECGL-30) was used as the excitation source, and the incident laser power was adjusted using a calibrated graded neutral density filter (Edmund Optics, U.S.A.). A notch filter was placed on the emission side to eliminate excitation laser scatter. The incident laser power density was typically adjusted to 0.28 W \cdot cm $^{-2}$ for the solution-phase measurements and 0.89 W \cdot cm $^{-2}$ for the solid-state samples.

An Edinburgh Instruments LP920 laser flash photolysis spectrometer was used to measure the triplet–triplet transient absorption kinetics and triplet decay of C_{60} used in the NCPU experiments. In brief, a flash-lamp-pumped, Q-switched Tempest 300 Nd:YAG laser producing 3–5 ns pulses and operating at a frequency of 10 Hz and a beam diameter of ~ 6 mm was used as the excitation source. Either the second-harmonic wavelength, 532 nm (≤ 180 mJ), or the third-harmonic wavelength, 355 nm (≤ 70 mJ), was used to excite the samples. The laser intensity incident on the sample was reduced by slightly defocusing the beam using a plano-concave lens (focal length = -13 mm, Edmund Optics); a typical average power density delivered to the sample cell was 0.67 W \cdot cm $^{-2}$ (19 mJ/pulse at 10 Hz).

The absorption spectrum and the time-dependent absorption kinetics of the transients formed upon excitation with the laser pulse were probed using a 450 W xenon arc lamp (Xe920) producing either continuous or pulsed (pulse duration ~ 0.5 –10 ms, repetition rate ~ 10 Hz) light in the 190–2600 nm spectral range. The excitation beam and the probe beam cross each other at 90° in a 10 mm \times 10 mm quartz cuvette containing the sample. The transmitted light is then focused onto a Czerny–Turner grating monochromator (TMS300) and finally detected using either an LP900 photomultiplier or an ICCD camera. The photomultiplier detector was used for taking kinetic data at a single wavelength in the 185–870 nm region and was supplemented by a Princeton PI-MAX ICCD camera that has a spectral detection range of 180–850 nm. A

digital oscilloscope (Tektronix TDS3032C, 300 MHz bandwidth) was used to record the real time signal from the detector. The time resolution of the instrument is ~ 7 ns. Data acquisition was facilitated using L900 software supplied by Edinburgh Instruments. This instrument was also used without the probe light source to measure the time evolution of the spectrum of DF in the photon upconversion experiments.

RESULTS AND DISCUSSION

Previously reported photophysical properties of the components of the donor–acceptor system used in NCPU experiments here are collected in Table 1. An is a particularly useful

Table 1. Photophysical Properties of C_{60} and an in Solution

properties	C_{60}	anthanthrene	refs
$E(S_n)^a$ (eV)	3.04		27
$E(S_1)$ (eV)	1.7	2.8	23, 31
$E(T_1)$ (eV)	1.5	1.4	18, 36, 37
$\tau(S_n)^a$ (ps)	0.20–0.25		22, 30
$\tau(S_1)$ (ns)	1.2	(2.8, 3.1–6.1 ^b)	22, 38, 31, 32, 39
$\tau(T_1)$ (ms)	0.14	0.11	24, 25, 39
η_{ISC} (direct excitation)	1.0	0.53–0.76 ^b	22, 31
ϕ_{ESI} (direct excitation)	3.2×10^{-4}	0.24–0.47 ^b	22, 31, 32

^a $n \approx 7$; lowest-energy electric-dipole-allowed excited electronic singlet state. ^bSolvent-dependent; cf. ref 31.

blue emitter to investigate for NCPU purposes for the following reasons. (i) An has a relatively large S_1 – S_0 fluorescence quantum yield (0.47 upon direct excitation in toluene³¹), and the major competing nonradiative process is intersystem crossing to T_1 , preserving triplet excitation when fluorescence does not occur. (ii) Its published T_1 state energy lies lower than that of C_{60} (by about 0.1 eV), making triplet–triplet energy transfer from C_{60} to An a thermodynamically favorable process. (iii) An's lowest excited singlet state has an energy equal to almost exactly twice its triplet energy and is reached from the ground state by an electric-dipole-allowed one-photon transition. Using Nickel's empirical assessment,²⁶ the probability of forming its fluorescent S_1 state by homomolecular TTA should be large, with minimal thermal energy loss. (iv) Substitution of the An ring system can be used to systematically tune its electronic energies and photophysical properties.³¹

Johannessen et al.³⁷ have reported the most thorough study of An's UV–visible absorption spectrum. They assign its lowest-energy absorption band in the violet to a ${}^1B_{2u}$ – ${}^1A_{1g}$ electric-dipole-allowed transition that exhibits a slight red shift in solvents of increasing polarizability. They also predict, using a quantum chemical linear combination of orthogonal atomic orbitals (LCOAO) model, that a second ${}^1B_{2u}$ state is located only a few hundred wavenumbers higher in energy from S_1 and find substantial experimental evidence for it from solvent and temperature shifts. This study does not alter the data presented in Table 1 but does provide some additional cautionary information to consider when discussing the energy-transfer dynamics in An-containing systems. In particular, although the location of T_1 in An at 1.4 eV is well-established, the location of the second triplet state (which should be near T_1) and its influence on the relevant triplet energy-transfer processes are unknown.

Zhao et al.^{40–43} have recently demonstrated that dyads of C_{60} with bodipy or naphthalenediimide can be used as efficient triplet sensitizers for NCPU. They also showed that the system of unsubstituted C_{60} sensitizer with perylene (P) as the triplet acceptor/annihilator exhibits NCPU of relatively low efficiency due primarily to the weak molar absorptivity of C_{60} in the 400–600 nm region. The relative energies of the triplets of the donor and acceptor also determine TTA efficiency. In the C_{60} + P system, these energies are almost equal,^{23,44} resulting in a primarily entropic driving force for triplet–triplet energy transfer prior to annihilation in triplet P.^{14,45,46} In this respect, An should be a better energy acceptor from triplet C_{60} because its slightly lower triplet energy (ΔE of ~ 0.1 eV) should result in a 50-fold reduction in the rate of activated (enthalpic) back-energy transfer at room temperature in the triplet donor–acceptor energy-transfer pair.

The absorption spectra of C_{60} and An in toluene (Figure S1, Supporting Information (SI)) are identical to previously reported solution-state spectra.^{23,27,31,32} Examination of the absorption spectrum of An in the 15 000–21 000 cm^{-1} region in greater detail (inset Figure S1, SI) shows that the absorbance of An is close to zero at 532 nm ($18\,800\text{ cm}^{-1}$), the excitation wavelength used for the NCPU experiments in toluene. The absorption spectra of a constant concentration of C_{60} in toluene with varying concentrations of An were also measured. The absorption spectra of An alone in toluene at each of the measured concentrations were then subtracted from the corresponding mixture spectra of C_{60} and An. The resulting difference spectra exhibit no significant changes in spectral band shape or in peak intensity, and no additional bands were observed. These difference spectra suggest that the ground-state association between C_{60} and An is negligible in toluene at the concentrations employed in the NCPU experiments. Clean excitation of C_{60} alone is therefore expected at 532 nm, where its molar extinction coefficient in toluene is $1.1 \times 10^3\text{ M}^{-1}\text{ cm}^{-1}$.

The fluorescence spectra (Figure S2, SI) of C_{60} and An excited separately also reproduced the corresponding prompt one-photon-excited fluorescence spectra in solution reported in the literature^{23,31,32} (when corrected for background scatter from the solvent, fluorescence reabsorption effects, and the variation of the detector sensitivity with wavelength^{14,34,35}). Note that the emission spectrum of C_{60} extends into the near-IR region and has negligible overlap with the fluorescence of An located at shorter wavelengths.

Upconverted S_1 fluorescence from An mixed with C_{60} in toluene was observed upon both cw and pulsed excitation of the C_{60} at 532 nm. Figure 1 shows the temporal evolution of the emission following nanosecond pulsed laser excitation. The DF spectrum of An in these donor–acceptor experiments closely resembles the one-photon-excited prompt fluorescence spectrum of An^{31,32} in similar solvents except for the segment of the spectrum at $\lambda < 425$ nm, where fluorescence reabsorption effects are significant. Figure 2A shows how the intensity of upconverted fluorescence varies with incident cw laser power for a fixed solution composition. The blue side of the raw upconverted fluorescence spectrum is slightly red-shifted compared to the prompt one-photon-excited S_1 fluorescence spectrum of An owing to emission reabsorption by both C_{60} and An. All emission spectra were corrected for this artifact and for the effects of solvent background scatter using the method reported previously.^{14,34,35} Even with these standard corrections, strong emission reabsorption by An

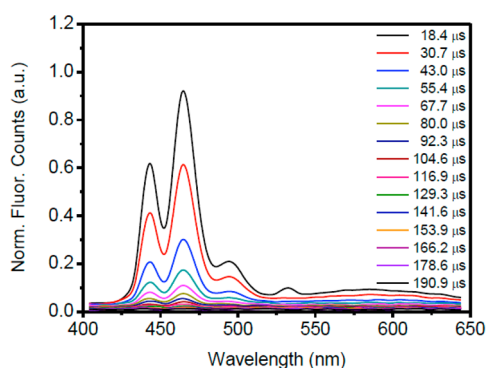


Figure 1. Time-resolved DF spectra obtained by 5 ns pulsed laser excitation of 1.0×10^{-4} M C_{60} and 1.0×10^{-4} M An in toluene at 532 nm.

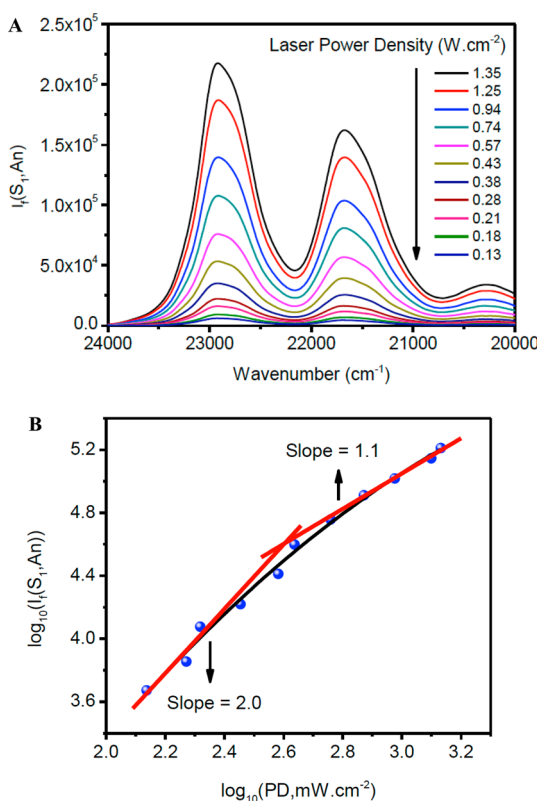


Figure 2. (A) Upconverted fluorescence spectrum of an equimolar mixture of An and C_{60} (1.0×10^{-4} M) in toluene as a function of incident cw laser power density. (B) Double logarithmic plot of the data in (A). All of the samples were excited with a cw 532 nm laser, the excitation monochromator bandwidth was fixed at 2.0 nm, and the emission band-pass was fixed at 4.0 nm. Slopes are from tangents to the curve at the terminal data points.

(and to some extent by C_{60}) clearly distorted the (0–0) vibronic region of the An emission spectra from 22 000 to 24 000 cm^{-1} (cf. Figure S3, SI), particularly at high An concentrations. Therefore, the peak spectral intensity of the second emission band of An at 21 650 cm^{-1} (462 nm) was used for further analysis. As expected, no upconverted fluorescence was observed from air-saturated C_{60} + An solutions in toluene owing to quenching of the triplet states of C_{60} and An by molecular oxygen. In addition, solutions of C_{60} or An alone in toluene excited at 532 nm showed no upconverted emission in the visible region under otherwise identical experimental

conditions (although weak DF from C_{60} alone is observed in the far red and a small amount of two-photon-excited prompt fluorescence is seen from An alone). These control experiments indicate that the upconverted fluorescence observed from the C_{60} + An solutions is due to one-photon absorption by C_{60} and triplet–triplet energy transfer followed by homomolecular TTA in An.

To verify that the fluorescence observed from An with added C_{60} is due to the TTA process, a double logarithmic plot of the observed fluorescence intensity from a solution containing fixed concentrations of C_{60} and An in toluene versus the incident laser power density was prepared, as shown in Figure 2B. The standard kinetic model of TTA^{24,47} predicts that these plots will produce a slope close to 2 in the low-power range and that the slopes will decrease to a value close to 1 with increasing power. The expected trend is observed here. At the low-power threshold, kinetically first-order triplet deactivation processes (i.e., intramolecular relaxation of the triplet state to the ground singlet state through either radiative or nonradiative channels and pseudo-first-order quenching) dominate, resulting in a slope close to 2. However, at higher laser powers, annihilation dominates due to the high triplet concentrations, resulting in a slope closer to 1.^{47–49} Because the laser power corresponding to the region of deviation from a slope of 2 is reported to result in the highest TTA efficiency on a per absorbed photon basis,^{48,49} a laser power density of 0.28 $\text{W}\cdot\text{cm}^{-2}$ was used for most additional steady-state upconversion measurements.

The net efficiency of NCPU is also a function of the concentration of An (cf. Figure S4, SI). At the concentrations of An and C_{60} used in Figure 2 (each at 1×10^{-4} M), the use of previously measured rate constants with the standard kinetic model predicts that a substantial fraction of $^3C_{60}$ formed by photon absorption at 532 nm will be quenched by triplet–triplet energy transfer to An. At substantially higher An concentrations and constant laser power density, the intensity of upconverted fluorescence levels off as the probability of triplet–triplet energy transfer reaches a maximum and then decreases, likely due to self-quenching of the product excited singlet state by ground-state An. Thus, although An is an excellent choice as a triplet acceptor and upconverter due to the location of its T_1 and S_1 energies relative to those of C_{60} , self-quenching of its TTA product state, S_1 , results in a small loss of absorbed photon energy at optimum An concentrations.

The $T_1 \rightarrow T_n$ transient absorption spectrum of 1×10^{-4} M C_{60} in toluene excited at 532 nm (Figure S5, SI) is similar to the spectra reported previously in the literature.^{22,50,51} The spectral band at 750 nm, which has a molar absorptivity²² of 16 100 $\text{M}^{-1} \text{cm}^{-1}$, was used to measure the transient decay kinetics of the C_{60} triplets (cf. inset Figure S5, SI). The decay rates measured under our conditions (vide infra) are very similar to the decay rates of $^3C_{60}$ in toluene measured by Fujitsuka and Ito²² but yield lifetimes that are shorter than those obtained by Weisman (133 μs) under conditions that suppressed bimolecular processes.²⁵

Figure 3A shows the time-resolved triplet transient absorption spectra of C_{60} excited at 532 nm in the presence of An. The spectra exhibit band maxima at 750 nm due to $^3C_{60}$ and at 418, 838, and 858 nm due to excited An. The steady-state absorption spectrum of An exhibits intense features at 408 and 438 nm, and as expected, the transient absorption spectra show bleaching at these wavelengths. The inset of Figure 3A shows the temporal evolution of the transient signals observed at 418, 438, 750, and 858 nm. The transient decay due to triplet

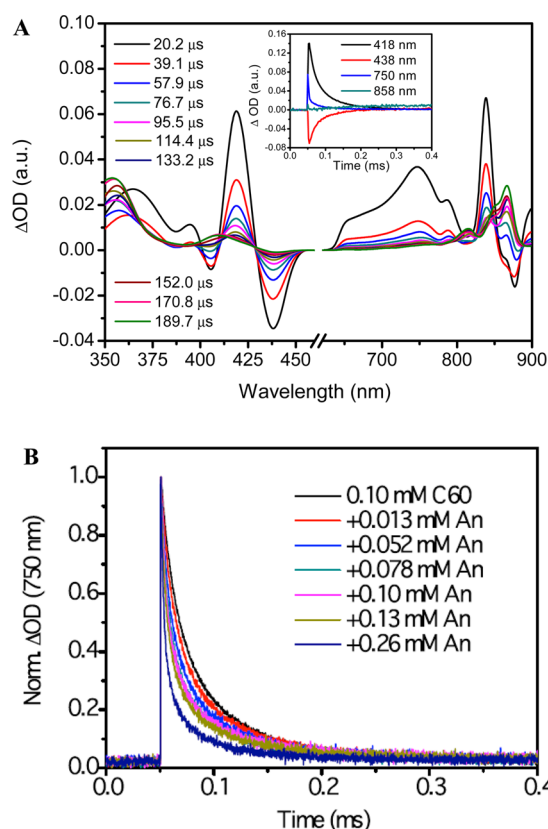
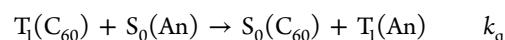
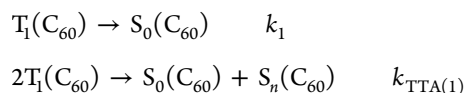


Figure 3. (A) $T_1 \rightarrow T_n$ transient absorption spectrum of 1×10^{-4} M C_{60} + 5.2×10^{-4} M An in toluene excited at 532 nm. The inset shows the transient signals measured at 418, 438, 750, and 858 nm. (B) Transient absorption decay of 1.0×10^{-4} M C_{60} at 750 nm measured as a function of An concentration. The laser pulse width was 5 ns, and the laser power density at the sample was $0.67 \text{ W} \cdot \text{cm}^{-2}$.

An observed at 418 nm and the rise at 438 nm (due to repopulating the ground state of An) occur on the same 100 μs time scale and exhibit similar but inverted profiles, consistent with their assignments and confirming that the triplet state of An is the longest-lived reservoir for excitation energy in the An + C_{60} mixtures. The feature observed at 750 nm (due to the T_1 state of C_{60}) exhibits a decay profile that becomes shorter-lived and is quenched with increasing An concentration. Figure 3B shows greater detail of the time dependence of the normalized triplet C_{60} absorption with added An when monitoring its transient spectrum at 750 nm. The signals at 418, 438, and 750 nm are straightforward to interpret and provide all of the needed kinetic data for both the donor and acceptor in this system. Deconvolution of the signals at 408 nm and in the near-infrared were therefore not pursued.

The 800 cm^{-1} spacing between the zero-point energies of the triplets of C_{60} and An results in a population of thermally activated An triplets lying above the zero-point energy of $^3C_{60}$ that is less than 2% of the total population at room temperature. Under these conditions, triplet–triplet back-energy transfer will not contribute significantly to the overall $T_1(C_{60})$ kinetics. If recycling of $S_n(C_{60})$ to $T_1(C_{60})$ is neglected, then the mechanism of triplet C_{60} decay can be satisfactorily represented by



where k_1 represents the sum of the rate constants for all parallel first-order and pseudo-first-order processes by which triplet C_{60} can decay under the chosen experimental conditions. On the basis of this mechanism, the rate of decay of triplet C_{60} (following initial photon excitation and rapid, quantitative intersystem crossing) will then be given by^{45,52}

$$\frac{d[T_1(C_{60})]_t}{dt} = -k_1[T_1(C_{60})]_t - k_{TTA(1)}[T_1(C_{60})]_t^2 - k_q[T_1(C_{60})]_t[S_0(\text{An})]_t \quad (1)$$

which, at $t = 0$, leads to

$$\frac{\left. \frac{d[T_1(C_{60})]_t}{dt} \right|_0}{[T_1(C_{60})]_0} = -\{(k_1 + k_q[S_0(\text{An})]_0) + k_{TTA(1)}[T_1(C_{60})]_0\} \quad (2)$$

Following the method of Schmidt et al.,^{45,52} values of $(k_1 + k_q[S_0(\text{An})]_0)$ and $k_{TTA(1)}$ can be obtained by fitting the early part of the normalized decays shown in Figure 3B using eq 2 (cf. data summarized in Table S1, SI). A graph of $(k_1 + k_q[S_0(\text{An})]_0)$ versus $[S_0(\text{An})]$ is shown in Figure 4. This plot

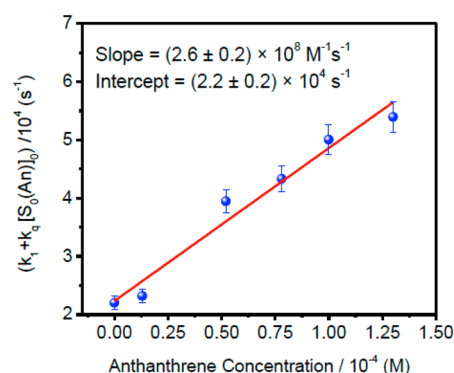
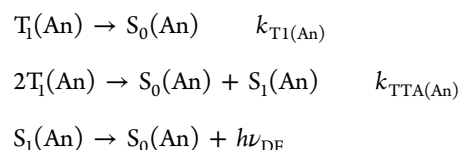


Figure 4. Dependence of the quasi-first-order rate constants of the decay of $^3C_{60}$ on the concentration of added An. The fit to the data is according to an equation derived based on the mechanism proposed by Schmidt et al.⁴⁵ $R^2 = 0.96$ for the least-squares fit.

provides the rate constants $k_1 = (2.2 \pm 0.2) \times 10^4 \text{ s}^{-1}$ and $k_q = (2.6 \pm 0.2) \times 10^8 \text{ M}^{-1} \text{ s}^{-1}$. The value of k_1 is similar to those found previously for the first-order decay of $^3C_{60}$ under similar conditions, whereas k_q is a factor of ~ 40 smaller than the diffusion-controlled quenching rate constant $k_d = 1.1 \times 10^{10} \text{ M}^{-1} \text{ s}^{-1}$. The value of $k_{TTA(1)}$ obtained from these data is $(2.5 \pm 0.3) \times 10^9 \text{ M}^{-1} \text{ s}^{-1}$ and lies between two previous measurements by Fujitsuka and Ito²² ($1.1 \times 10^9 \text{ M}^{-1} \text{ s}^{-1}$) and by Ebbesen et al.³⁸ ($\geq 4.8 \times 10^9 \text{ M}^{-1} \text{ s}^{-1}$).

After triplet–triplet energy transfer from $^3C_{60}$, triplet An will decay via the processes



where, again, $k_{T1(\text{An})}$ represents the sum of the rate constants for all parallel first-order and pseudo-first-order processes by which triplet An can decay under the chosen experimental

conditions. Ignoring any self-quenching of the fluorescing S_1 state of An and recycling its T_1 state via S_1 – T_1 intersystem crossing, the temporal evolution of the intensity of the DF from An in the An + C_{60} upconversion experiments (cf. Figure 1) can be related to the triplet An concentrations by the equations^{28,52}

$$\frac{d\sqrt{I_{DF}(t)}}{dt} = \sqrt{C} \frac{d[T_1(\text{An})]_t}{dt} = -k_{T1(\text{An})}[T_1(\text{An})]_t - k_{TTA(\text{An})}[T_1(\text{An})]_t^2 \quad (3)$$

where C is a proportionality constant. Equation 3 has the solution

$$\frac{[T_1(\text{An})]_t}{[T_1(\text{An})]_0} = \frac{1 - \beta}{e^{k_{T1(\text{An})}t} - \beta} \quad (4)$$

where β is the fraction of An triplets that decay via TTA and is given in this case by $\beta = k_{TTA(\text{An})}[T_1(\text{An})]_0 / (k_{T1(\text{An})} + k_{TTA(\text{An})}[T_1(\text{An})]_0)$.²⁸ Fits of the square root of the normalized DF intensity using eqs 3 and 4 resulted in values of β approaching 1, indicating that TTA in An is close to the strong annihilation limit in these experiments.²⁸ A representative fit is shown in Figure 5. Averaging over several data sets in the

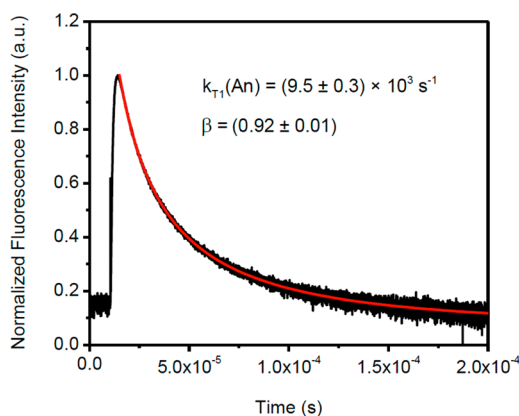


Figure 5. Fit of the square root of the normalized DF from 1.0×10^{-4} M C_{60} + 7.8×10^{-4} M An in toluene using eqs 3 and 4. The best fit was determined by minimizing the reduced χ^2 value.

intermediate An concentration range (to minimize self-quenching effects) yielded a rate constant of $k_{T1(\text{An})} = (9.5 \pm 0.3) \times 10^3 \text{ s}^{-1}$ and a value of $\beta = (0.92 \pm 0.01)$. This calculated first-order decay rate constant of triplet An yields a lifetime of $(1.1 \pm 0.3) \times 10^{-4} \text{ s}$, in excellent agreement with a previous measurement³⁹ (cf. Table 1).

With values of β approaching 1, the fraction of An triplets decaying by first-order kinetic processes can be ignored with only small systematic error, in which case eq 4 may be reduced to²⁸

$$\frac{[T_1(\text{An})]_t}{[T_1(\text{An})]_0} = \frac{1}{1 + K_A t} \quad (5)$$

where $K_A = k_{TTA(\text{An})}[T_1(\text{An})]_0$. Fitting the square root of the DF intensity using eqs 3 and 5 can then, in principle, yield the rate constant for homomolecular TTA in triplet An. Figure 6 shows the fit of eq 5 to the observed DF from C_{60} + An, which yields a value of $K_A = (1.4 \pm 0.1) \times 10^5 \text{ s}^{-1}$.

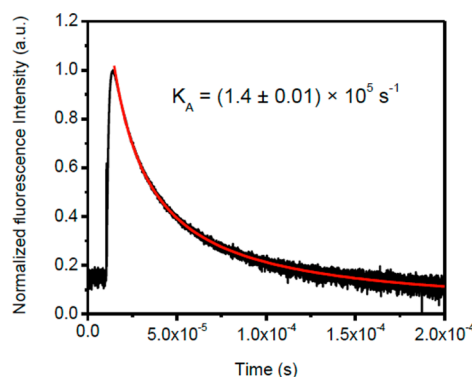


Figure 6. Square root of the normalized DF intensity from 1.0×10^{-4} M C_{60} + 7.2×10^{-4} M An in toluene using eqs 3 and 5. The best fit was obtained by minimizing the calculated reduced χ^2 value.

An estimate of the rate constant for homomolecular TTA in An can be obtained from this value of K_A if the corresponding concentration of triplet An at $t = 0$ can be estimated. An upper limit can be obtained from the initial concentration of triplet C_{60} . Its initial transient absorbance at 750 nm where the molar absorptivity is known was measured. Knowing that the absorbance path length in the laser flash system is approximately 0.6 cm then yields $[T_1(C_{60})]_0 \approx 1.3 \times 10^{-5} \text{ M}$ for the conditions under which the data of Figure 6 were obtained. Thus, the maximum concentration of An triplets will be $\sim 1.2 \times 10^{-5} \text{ M}$ at $\beta = 0.92$, leading to $k_{TTA(\text{An})} \approx 1.1 \times 10^{10} \text{ M}^{-1} \text{ s}^{-1}$, very close to the computed diffusion-controlled limit of $1.1 \times 10^{10} \text{ M}^{-1} \text{ s}^{-1}$. This value is likely to be overestimated because it implies that there is no spin-statistical limit to the TTA process in An, an unlikely scenario even though Schmidt has measured TTA efficiencies on the order of 60%.⁵² Approximations noted above will introduce some systematic error into this estimate but are somewhat offset by the fact that the C_{60} solutions employed are optically thin at 532 nm so that the initial concentration of $^3C_{60}$ is more uniformly spatially distributed in the irradiation cell, unlike previous measurements.⁵² Nevertheless, the fact that homomolecular TTA in An precisely fits Nickel's criteria²⁶ for favorable singlet-state population by TTA suggests that a value of $k_{TTA(\text{An})}$ not too far removed from the diffusion limit may be possible. Moreover, the second low-lying triplet state of An (vide supra) is likely to come into play when its triplet–triplet encounters do not proceed via the upconversion singlet product channel, and Schmidt has suggested that this situation can result in an efficiency in excess of the usual spin-statistical limit.^{47,52} We are pursuing this line of investigation.

Finally, in order to demonstrate the potential utility of An as a blue emitter in NCPUs, we have compared the upconverted fluorescence intensities obtained from solutions of C_{60} and An with those from C_{60} and P under identical conditions, as shown in Figure 7. Despite P's larger S_1 – S_0 fluorescence quantum yield ($\phi_f \approx 0.8$),⁵³ the solution-phase DF originating from C_{60} + An is about 10 times more intense than that from C_{60} + P up to approximately millimolar concentrations of the blue emitter. At still higher acceptor concentrations, we postulate that singlet self-quenching of An reduces its NCPU emission intensity. In fact bright, blue upconverted fluorescence is observable with the naked eye from degassed solutions of C_{60} in toluene containing only micromolar concentrations of An (see Figure S7, SI) but not in C_{60} solutions containing similar concentrations of P. As discussed

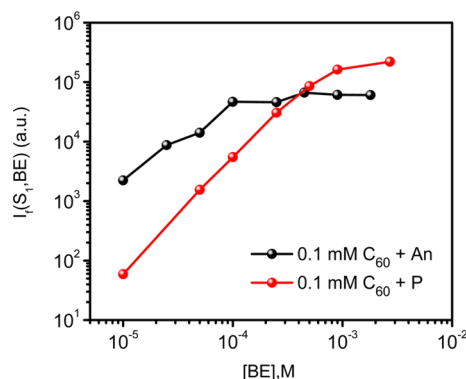


Figure 7. Comparison of the delayed emission intensities observed at 470 nm for 1.0×10^{-4} M C_{60} mixed with An or P. The samples were excited at 532 nm, and the emission bandwidth was fixed at 0.4 nm. The laser power density was $0.28 \text{ W} \cdot \text{cm}^{-2}$.

above, this enhanced upconverted emission efficiency can be attributed to the favorable enthalpic driving force for the energy transfer in the C_{60} + An system⁴⁵ and to the high rate of formation of product singlet states via homomolecular TTA in An.

Finally, in order to demonstrate the feasibility of using the C_{60} + An system to generate upconverted emission in the solid state, we have carried out initial measurements of NCPU in a PMMA solid matrix. Samples were prepared as described in the Experimental Section and were covered with a thin layer of polyvinyl alcohol, which acts as a barrier to molecular oxygen, thus reducing diffusive quenching.¹⁰ Figure 8 shows the prof-

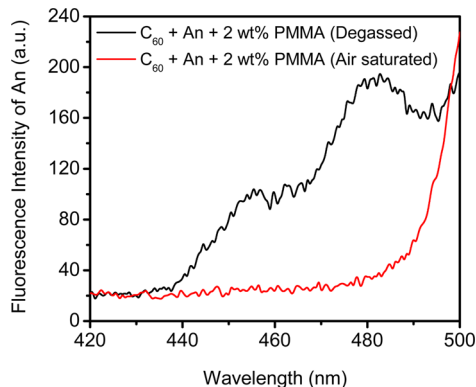


Figure 8. Upconverted S_1 emission observed from a thin PMMA film prepared from a solution of An and C_{60} + 2.0 wt % PMMA excited at 532 nm at $0.89 \text{ W} \cdot \text{cm}^{-2}$. The emission bandwidth was 6 nm.

of-principle experiment in which upconverted fluorescence is observed from a sample containing a thin layer of C_{60} (2 mM in solution), An (1 mM in solution), and 2 wt % PMMA on a glass slide, degassed and excited at 532 nm. The emission spectrum is distorted due to reabsorption by An but nevertheless is similar to the solution-phase DF spectrum. (Scatter from the excitation laser is visible toward the 500 nm region.) A spectrum of the same sample taken under identical experimental conditions except that that it was air-saturated showed no emission in the 400–500 nm range, confirming that the emission observed from the degassed sample is in fact due to the NCPU process in C_{60} + An. The intensity of fluorescence from the thin film sample is much lower than the emission from the solution-phase samples, consistent with

the much lower absorbance of the film and the fact that TTA in solid matrixes primarily proceeds through exciton annihilation, the rate of which largely depends upon the state of aggregation of the sensitizer and the emitter. Finally, C_{60} + P in a similar PMMA thin film did not produce measurable upconverted emission for a range of C_{60} and P concentrations employed. We ascribe this difference to the reasons enumerated above for the solution-phase experiments and perhaps to poorer aggregation between C_{60} and P in the PMMA films.

CONCLUSIONS

Recent publications have demonstrated that several factors control the efficiency of NCPU. The need for sensitizers and acceptors having appropriate triplet energies has been emphasized here, where we show that employing even a poor absorber such as C_{60} may still give rise to a reasonable net NCPU quantum efficiency if the acceptor is chosen so as (i) to favor forward triplet energy transfer, (ii) to suppress back-energy transfer, and (iii) to favor forming the radiant product singlet state by homomolecular TTA. We have compared the mechanism and kinetics of low-power NCPU in two sensitizer + blue emitter systems in nonpolar toluene solution. In C_{60} + An, the triplet energy of An is lower than that of C_{60} , favoring net exergonic forward triplet–triplet energy transfer. An's fluorescent S_1 state is located at an energy close to double the energy of its annihilating T_1 state, increasing the probability of yielding upconverted fluorescence. In C_{60} + P, a well-researched system, the similar triplet energies of C_{60} and P produce a largely entropically driven triplet–triplet energy transfer of lower net efficiency. In addition, TTA in An is found to be very efficient with a rate constant of $\sim 10^{10} \text{ M}^{-1} \text{ s}^{-1}$. This combination of factors results in an order of magnitude larger DF intensity for the C_{60} + An system compared to that of C_{60} + P at moderate blue emitter concentrations in solution. Finally, we have observed NCPU in C_{60} + An thin PMMA films under conditions where a similar C_{60} + P system in PMMA produces no observable DF. The robustness of fullerenes under environmental conditions has prompted us to continue these explorations, with the objective of improving the net energy conversion efficiencies and longevity of solar photovoltaic cells.

ASSOCIATED CONTENT

Supporting Information

The following data are provided in the accompanying Supporting Information: (i) a table of values of rate constants for the relaxation of the triplet state of C_{60} as a function of An concentration; (ii) absorption spectra of C_{60} and An; (iii) fluorescence spectra of C_{60} and An; (iv) uncorrected fluorescence upconversion spectra of C_{60} plus varying concentrations of An; (v) double logarithmic plot of the relative intensity of delayed upconverted fluorescence from An as a function of An concentration; (vi) time-resolved transient absorption spectra of C_{60} in toluene; (vii) time-resolved delayed upconverted fluorescence of An as a function of An concentration; and (viii) a photograph of upconverted DF of An from C_{60} + An in toluene excited at 532 nm. This material is available free of charge via the Internet at <http://pubs.acs.org>.

AUTHOR INFORMATION

Corresponding Author

*E-mail: ron.steer@usask.ca (R.P.S.); matthew.paige@usask.ca (M.F.P.); sunishks@gmail.com (S.K.S.).

Present Address

[§]S.K.S.: Department of Physics, Durham University, Durham, United Kingdom DH1 3LE.

Notes

The authors declare no competing financial interest.

ACKNOWLEDGMENTS

The authors wish to thank the Natural Sciences and Engineering Research Council of Canada for their continuing support of this research. Instrumentation purchased in part from a grant from Western Economic Diversification Canada is also gratefully acknowledged.

REFERENCES

- (1) Lissau, J. S.; Gardner, J. M.; Morandeira, A. Photon Upconversion on Dye-Sensitized Nanostructured ZrO_2 Films. *J. Phys. Chem. C* **2011**, *115* (46), 23226–23232.
- (2) Cheng, Y. Y.; Fucel, B.; MacQueen, R. W.; Khoury, T.; Clady, R.; Schulze, T. F.; Ekins-Daukes, N. J.; Crossley, M. J.; Stannowski, B.; Lips, K.; Schmidt, T. W. Improving the Light-Harvesting of Amorphous Silicon Solar Cells with Photochemical Upconversion. *Energy Environ. Sci.* **2012**, *5* (5), 6953–6959.
- (3) Schulze, T. F.; Cheng, Y. Y.; Fucel, B.; MacQueen, R. W.; Danos, A.; Davis, N.; Tayebjee, M. J. Y.; Khoury, T.; Clady, R.; Ekins-Daukes, N. J.; Crossley, M. J.; Stannowski, B.; Lips, K.; Schmidt, T. W. Photochemical Upconversion Enhanced Solar Cells: Effect of a Back Reflector. *Aust. J. Chem.* **2012**, *65* (5), 480–485.
- (4) Schulze, T. F.; Czolk, J.; Cheng, Y. Y.; Fucel, B.; MacQueen, R. W.; Khoury, T.; Crossley, M. J.; Stannowski, B.; Lips, K.; Lemmer, U.; Colmann, A.; Schmidt, T. W. Efficiency Enhancement of Organic and Thin-Film Silicon Solar Cells with Photochemical Upconversion. *J. Phys. Chem. C* **2012**, *116*, 22794–22801.
- (5) Chiang, C.; Kimyonok, A.; Etherington, M. K.; Griffiths, G. C.; Jankus, Y.; Turksoy, F.; Monkman, A. P. Ultrahigh Efficiency Fluorescent Single and Bi-Layer Organic Light Emitting Diodes: The Key Role of Triplet Fusion. *Adv. Funct. Mater.* **2012**, 1–8.
- (6) Jankus, Y.; Chiang, C.; Dias, F.; Monkman, A. P. Deep Blue Exciplex Organic Light-Emitting Diodes with Enhanced Efficiency; P-type or E-type Triplet Conversion to Singlet Excitons? *Adv. Mater.* **2013**, 1–5.
- (7) Miteva, T.; Yakutkin, V.; Nelles, G.; Balushev, S. Annihilation Assisted Upconversion: All-Organic, Flexible and Transparent Multicolour Display. *New J. Phys.* **2008**, *10*, 103002.
- (8) Wohnhaas, C.; Turshatov, A.; Mailander, V.; Lorenz, S.; Balushev, S.; Miteva, T.; Landfester, K. Annihilation Upconversion in Cells by Embedding the Dye System in Polymeric Nanocapsules. *Macromol. Biosci.* **2011**, *11* (6), 772–778.
- (9) Kim, J.-H.; Kim, J.-H. Encapsulated Triplet–Triplet Annihilation-Based Upconversion in the Aqueous Phase for Sub-Band-Gap Semiconductor Photocatalysis. *J. Am. Chem. Soc.* **2012**, *134*, 17478–17481.
- (10) Sugunan, S. K.; Paige, M. F.; Steer, R. P. Determination of Oxygen Permeabilities in Thin Polymer Films using Quenching of Upconverted Fluorescence in Porphyrins. *Can. J. Chem.* **2011**, *89* (2), 195–202.
- (11) Lee, J.; Jadhav, P.; Reusswig, P. D.; Yost, S. R.; Thompson, N. J.; Congreve, D. N.; Hontz, E.; van Voorhis, T.; Baldo, M. A. Singlet Excitation Fission Photovoltaics. *Acc. Chem. Res.* **2013**, *46*, 1300–1311.
- (12) Shockley, W.; Quieser, H. J. Detailed Balance Limit of Efficiency of p–n Junction Solar Cells. *J. Appl. Phys.* **1961**, *32* (3), 510–519.
- (13) Singh-Rachford, T. N.; Castellano, F. N. Photon Upconversion Based on Sensitized Triplet–Triplet Annihilation. *Coord. Chem. Rev.* **2010**, *254*, 2560–2573.
- (14) Sugunan, S. K.; Tripathy, U.; Brunet, S. M. K.; Paige, M. F.; Steer, R. P. Mechanisms of Low-Power Noncoherent Photon Upconversion in Metalloporphyrin–Organic Blue Emitter Systems in Solution. *J. Phys. Chem. A* **2009**, *113* (30), 8548–8556.
- (15) Maiti, M.; Danger, B. R.; Steer, R. P. Photophysics of Soret-Excited Tetrapyrroles in Solution. IV. Radiationless Decay and Triplet–Triplet Annihilation Investigated Using Tetraphenylporphyrinato Sn(IV) . *J. Phys. Chem. A* **2009**, *113* (42), 11318–11326.
- (16) O'Brien, J. A.; Rallabandi, S.; Tripathy, U.; Paige, M. F.; Steer, R. P. Efficient S₂ State Production in ZnTPP-PMMA Thin Films by Triplet–Triplet Annihilation: Evidence of Solute Aggregation in Photon Upconversion Systems. *Chem. Phys. Lett.* **2009**, *475*, 220–222.
- (17) Yeow, E. K.; Ziolk, M.; Karolczak, J.; Shevyakov, S. V.; Alsato, A. E.; Maciejewski, A.; Steer, R. P. Sequential Forward S₂–S₂ and Back S₁–S₁ (Cyclic) Energy Transfer in a Novel Azulene–Zinc Porphyrin Dyad. *J. Phys. Chem. A* **2004**, *108* (50), 10980–10988.
- (18) Mataga, N.; Chosrowjan, H.; Shibata, Y.; Yoshida, N.; Osuka, A.; Kikuzawa, T.; Okada, T. First Unequivocal Observation of the Whole Bell-Shaped Energy Gap Law in Intramolecular Charge Separation from S₂ Excited State of Directly Linked Porphyrin–Imide Dyads and Its Solvent Polarity Dependencies. *J. Am. Chem. Soc.* **2001**, *123* (49), 12422–12423.
- (19) Sugunan, S. K.; Robotham, B.; Sloan, R. P.; Szymkowski, J.; Ghigginio, K. P.; Paige, M. F.; Steer, R. P. Photophysics of Untethered ZnTPP–Fullerene Complexes in Solution. *J. Phys. Chem. A* **2011**, *115*, 12217–12227.
- (20) Danger, B. R.; Bedient, K.; Maiti, M.; Burgess, I. J.; Steer, R. P. Photophysics of Self-Assembled Zinc Porphyrin–Bidentate Diamine Ligand Complexes. *J. Phys. Chem. A* **2010**, *114* (41), 11471–11476.
- (21) Harvey, P. D.; Bregier, F.; Aly, S. M.; Szymkowski, J.; Paige, M. F.; Steer, R. P. Dendron to Central Core S₁–S₁ and S₂–S_n ($n > 1$) Energy Transfers in Artificial Special Pairs Containing Dendrimers with Limited Numbers of Conformations. *Chem.—Eur. J.* **2013**, *19* (13), 4352–4368.
- (22) Fujitsuka, M.; Ito, O. Photoexcitation Dynamics of Fullerenes. In *Encyclopedia of Nanoscience and Nanotechnology*; Nalwa, H. S., Ed.; American Scientific Publishers: Valencia, CA, 2004; Vol. 8, p 593.
- (23) Accorsi, G.; Armaroli, N. Taking Advantage of the Electronic Excited States of [60]-Fullerenes. *J. Phys. Chem. C* **2010**, *114*, 1385–1403.
- (24) Ausman, K. D.; Weisman, R. B. Kinetics of Fullerene Triplet States. *Res. Chem. Intermed.* **1997**, *23* (5), 431–451.
- (25) Fraelich, M. R.; Weisman, R. B. Triplet-States of C₆₀ and C₇₀ in Solution — Long Intrinsic Lifetimes and Energy Pooling. *J. Phys. Chem.* **1993**, *97* (43), 11145–11147.
- (26) Nickel, B. Delayed Fluorescence from Upper Excited Singlet States S_n ($n > 1$) of the Aromatic Hydrocarbons 1,2-Benzanthracene, Fluoranthrene, Pyrene, and Chrysene in Cyclohexane. *Helv. Chim. Acta* **1978**, *61* (15), 198–222.
- (27) Orlandi, G.; Negri, F. Electronic States and Transitions in C₆₀ and C₇₀ Fullerenes. *Photochem. Photobiol. Sci.* **2002**, *1*, 289–308.
- (28) Bachilo, S. M.; Weisman, R. B. Determination of Triplet Quantum Yields from Triplet–Triplet Annihilation Fluorescence. *J. Phys. Chem. A* **2000**, *104* (33), 7711–7714.
- (29) Salazar, F. A.; Fedorov, A.; Berberan Santos, M. N. A Study of Thermally Activated Delayed Fluorescence in C₆₀. *Chem. Phys. Lett.* **1997**, *271* (4–6), 361–366.
- (30) Stepanov, A. G.; Portelli-Oberli, M. T.; Sassara, A.; Chegui, M. Ultrafast Intramolecular Relaxation of C₆₀. *Chem. Phys. Lett.* **2002**, *358*, 516–522.
- (31) Shah, B. K.; Neckers, D. C.; Shi, J. M.; Forsythe, E. W.; Morton, D. Photophysical Properties of Anthanthrene-Based Tunable Blue Emitters. *J. Phys. Chem. A* **2005**, *109* (34), 7677–7681.
- (32) Shah, B. K.; Neckers, D. C.; Shi, J. M.; Forsythe, E. W.; Morton, D. Anthanthrene Derivatives as Blue Emitting Materials for Organic Light-Emitting Diode Applications. *Chem. Mater.* **2006**, *18* (3), 603–608.
- (33) Guldi, D. M.; Prato, M. Excited-State Properties of C₆₀ Fullerene Derivatives. *Acc. Chem. Res.* **2000**, *33* (10), 695–703.
- (34) Liu, X.; Yeow, E. K. L.; Velate, S.; Steer, R. P. Photophysics and Spectroscopy of the Higher Electronic States of Zinc Metal-

loporphyrins: A Theoretical and Experimental Study. *Phys. Chem. Chem. Phys.* **2006**, *8* (11), 1298–1309.

(35) Lukaszewicz, A.; Karolczak, J.; Kowalska, D.; Maciejewski, A.; Ziolk, M.; Steer, R. P. Photophysical Processes in Electronic States of Zinc Tetraphenylporphyrin Accessed on One- and Two-Photon Excitation in the Soret Region. *Chem. Phys.* **2007**, *331* (2–3), 359–372.

(36) Parac, M.; Grimme, S. A TDDFT Study of the Lowest Excitation Energies of Polycyclic Aromatic Hydrocarbons. *Chem. Phys.* **2003**, *292* (1), 11–21.

(37) Johannessen, C.; Gorski, A.; Waluk, J.; Spangt-Larsen, J. Electronic States of Anthanthrene: Linear and Magnetic Circular Dichroism, Fluorescence Anisotropy and Quantum Chemical Calculations. *Polycyclic Aromat. Hydrocarbons* **2005**, *25*, 23–45.

(38) Ebbesen, T. W.; Tanigaki, K.; Kuroshima, S. Excited-State Properties of C60. *Chem. Phys. Lett.* **1991**, *181* (6), 501–504.

(39) Carmichael, I.; Hug, G. L. A Note on the Total Depletion Method of Measuring Extinction Coefficients of Triplet–Triplet Transitions. *J. Phys. Chem.* **1985**, *89* (19), 4036–4039.

(40) Wu, W. H.; Zhao, J. Z.; Sun, J. F.; Guo, S. Light-Harvesting Fullerene Dyads As Organic Triplet Photosensitizers for Triplet–Triplet Annihilation Upconversions. *J. Org. Chem.* **2012**, *77* (12), 5305–5312.

(41) Yang, P.; Wu, W. H.; Zhao, J. Z.; Huang, D. D.; Yi, X. Y. Using C-60–Bodipy Dyads that Show Strong Absorption of Visible Light and Long-Lived Triplet Excited States as Organic Triplet Photosensitizers for Triplet–Triplet Annihilation Upconversion. *J. Mater. Chem.* **2012**, *22* (38), 20273–20283.

(42) Huang, D.; Zhao, J.; Wu, W.; Yi, X.; Yang, P.; Ma, J. Visible-Light-Harvesting Triphenylamine Ethynyl C60–Bodipy Dyads as Heavy-Atom-Free Organic Triplet Photosensitizers for Triplet–Triplet Annihilation Upconversion. *Asian J. Org. Chem.* **2012**, *1*, 264–273.

(43) Guo, S.; Sun, J. F.; Ma, L. H.; You, W. Q.; Yang, P.; Zhao, J. Z. Visible Light-Harvesting Naphthalenediimide (NDI)–C-60 Dyads as Heavy-Atom-Free Organic Triplet Photosensitizers for Triplet–Triplet Annihilation Based Upconversion. *Dyes Pigm.* **2013**, *96* (2), 449–458.

(44) Clarke, R. H.; Hochstrasser, R. M. Location and Assignment of Lowest Triplet State of Perylene. *J. Mol. Spectrosc.* **1969**, *32* (2), 309.

(45) Cheng, Y. Y.; Fuckel, B.; Khoury, T.; Clady, R.; Ekins-Daukes, N. J.; Crossley, M. J.; Schmidt, T. W. Entropically Driven Photochemical Upconversion. *J. Phys. Chem. A* **2011**, *115* (6), 1047–1053.

(46) Penconi, M.; Ortica, F.; Elisei, F.; Gentili, P. L. New Molecular Pairs for Low Power Non-Coherent Triplet–Triplet Annihilation Based Upconversion: Dependence on the Triplet Energies of Sensitizer and Emitter. *J. Lumin.* **2013**, *135*, 265–270.

(47) Cheng, Y. Y.; Khoury, T.; Clady, R.; Tayebjee, M. J. Y.; Ekins-Daukes, N. J.; Crossley, M. J.; Schmidt, T. W. On the Efficiency Limit of Triplet–Triplet Annihilation for Photochemical Upconversion. *Phys. Chem. Chem. Phys.* **2010**, *12* (1), 66–71.

(48) Monguzzi, A.; Mezyk, J.; Scotognella, F.; Tubino, R.; Meinardi, F. Upconversion-Induced Fluorescence in Multicomponent Systems: Steady-State Excitation Power Threshold. *Phys. Rev. B* **2008**, *78*, 19.

(49) Monguzzi, A.; Tubino, R.; Hoseinkhani, S.; Campione, M.; Meinardi, F. Low Power, Non-Coherent Sensitized Photon Upconversion: Modelling and Perspectives. *Phys. Chem. Chem. Phys.* **2012**, *14* (13), 4322–4332.

(50) Dimitrijevic, N. M.; Kamat, P. V. Triplet Excited-State Behavior of Fullerenes: Pulse-Radiolysis and Laser Flash-Photolysis of C60 and C70 in Benzene. *J. Phys. Chem.* **1992**, *96* (12), 4811–4814.

(51) Riggs, J. E.; Sun, Y. P. Optical Limiting Properties of [60]Fullerene and Methano[60]Fullerene Derivatives in Solution versus in Polymer Matrix: The Role of Bimolecular Processes and a Consistent Nonlinear Absorption Mechanism. *J. Phys. Chem. A* **1999**, *103* (4), 485–495.

(52) Cheng, Y. Y.; Fuckel, B.; Khoury, T.; Clady, R.; Tayebjee, M. J. Y.; Ekins-Daukes, N. J.; Crossley, M. J.; Schmidt, T. W. Kinetic

Analysis of Photochemical Upconversion by Triplet–Triplet Annihilation: Beyond Any Spin Statistical Limit. *J. Phys. Chem. Lett.* **2010**, *1* (12), 1795–1799.

(53) Murov, S. L. *Handbook of Photochemistry*; Marcel Dekker: New York, 1973; p 19.